HHS Public Access

Author manuscript

Dev Cell. Author manuscript; available in PMC 2023 February 07.

Published in final edited form as:

Dev Cell. 2022 February 07; 57(3): 361–372.e5. doi:10.1016/j.devcel.2021.12.016.

Bacterial peptidoglycan muropeptides benefit mitochondrial homeostasis and animal physiology by acting as ATP synthase agonists

Dong Tian, **Min Han***

Department of MCDB, University of Colorado at Boulder, Boulder, CO 80309, USA

Summary

The symbiotic relationship between commensal microbes and host animals predicts unidentified beneficial impacts of individual bacterial metabolites on animal physiology. Peptidoglycan fragments (muropeptides) from the bacterial cell wall are known for their roles in pathogenicity and for inducing host immune responses. However, the potential beneficial usage of muropeptides, from commensal bacteria, by the host needs exploration. We identified a striking role for muropeptides in supporting mitochondrial homeostasis, development and behaviors in *C. elegans*. We determined that the beneficial molecules are disaccharide muropeptides containing a short AA chain, and they enter intestinal-cell mitochondria to repress oxidative stress. Further analyses indicate that muropeptides execute this role by binding to and promoting the activity of ATP synthase. Therefore, given the exceptional structural conservation of ATP synthase, the role of muropeptides as a rare agonist of the ATP synthase presents a major conceptual modification regarding the impact of bacterial cell metabolites on animal physiology.

Graphical Abstract

*Lead contact/Corresponding author: mhan@colorado.edu.

Author Contribution

DT designed research, performed experiments, analyzed data and wrote the paper; M.H. supervised the study and edited the paper.

Supplemental Information:

Supplemental information can be found online.

Declaration of Interests

The University of Colorado has filed a provisional patent application partly based on results from this study (63/231,350).

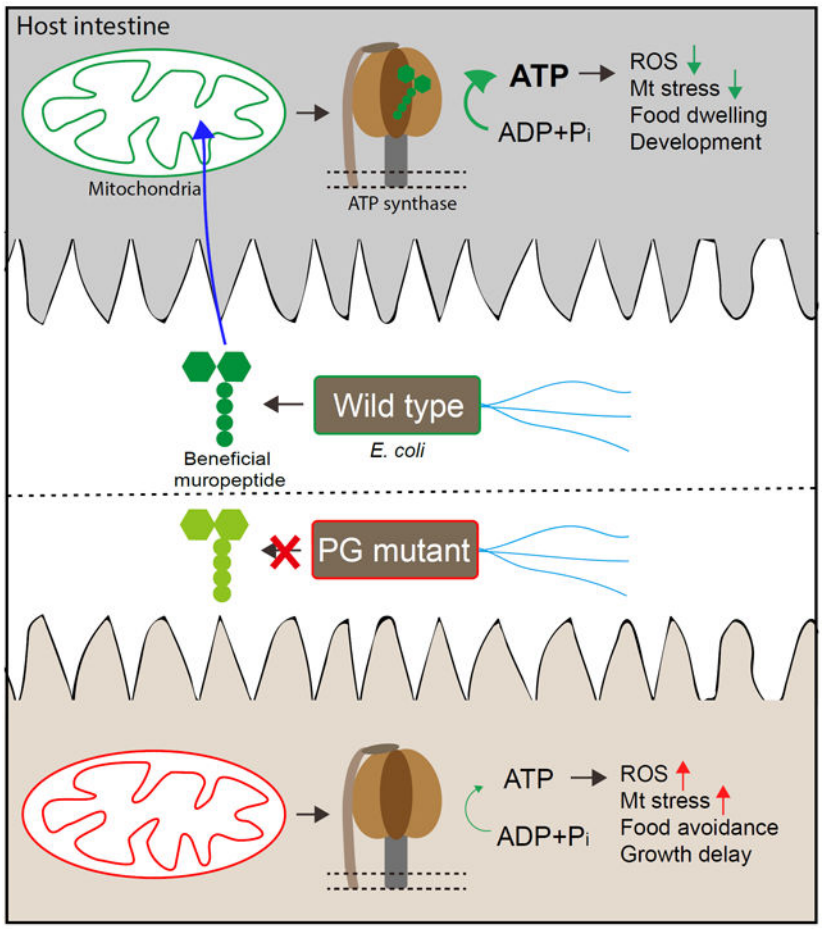

Keywords

bacteria cell wall; Muropeptides; PG fragments; PGN; ATP synthase; ATP synthase agonist; mitochondrial stress; unfolded protein response; UPR^{mt}; food avoidance; dwelling behavior

Introduction

A growing body of studies, mostly by high-throughput approaches, have revealed the enormously complexity and diversity of gut microbiota and their profound impact on a broad range of physiological functions in host animals (Barratt et al., 2017; Brown and Hazen, 2018; Fan and Pedersen, 2020; Kundu et al., 2017; Postler and Ghosh, 2017). Based on the “symbiosis” concept that describes the interdependent relationship between commensal microbes and host, animals have evolved various mechanisms to beneficially use many microbial metabolites to enhance their reproductive fitness. However, our understanding of these beneficial roles and the underlying mechanisms for individual microbial metabolites are still limited largely due to the challenging nature of studies using animal models (Cani, 2018). Therefore, developing effective animal models and new approaches to explore the role of individual microbial metabolites are highly desirable (Donia and Fischbach, 2015; Fischbach, 2018). The nematode *C. elegans* is an excellent model for dissecting the function

of bacterial metabolites on host physiology due to the merits for easy manipulation and defined microbiota (Garcia-Gonzalez et al., 2017; Heintz and Mair, 2014).

Peptidoglycan (PG) is a crucial and unique component of bacterial cell walls in both of Gram-positive and Gram-negative species (Schleifer and Kandler, 1972). The PG structure is made of a glycan backbone of repeating N-acetylglucosamine (NAG) and β-(1-4)-Nacetylmuramic acid (NAM) that are cross-linked by short peptides (Bourhis and Werts, 2007). During bacterial proliferation, up to 50% of PG is degraded by a turnover process (PG hydrolysis) that generates PG fragments with diverse structure known as muropeptides (Irazoki et al. 2019)(Park and Uehara 2008). Many of these PG breakdown products are also released into the environment, which is the intestine for commensal bacteria. Muropeptides are known to interact with host proteins for roles in bacterial pathogenicity and host innate immune responses (Humann and Lenz, 2009; Irazoki et al., 2019). Previous studies have shown that eukaryotes detect intact PG or its fragments by peptidoglycan recognition proteins (PGRPs) or Nod-like receptors (NLRs) (Girardin et al., 2003b; Gottar et al., 2002; McDonald et al., 2005). PG has been detected within animal cells, and high PG levels in animal cells were reported to correlate with most of the clinical manifestations of bacterial infections, such as fever, inflammation, septic shock, leukocytosis and arthritis (Palaniyar et al., 2002). However, some recent studies also suggested roles for PG molecules beyond pathogenicity and immune responses in animal hosts (Arentsen et al., 2018). The specific PG molecules involved in the beneficial impact on animal physiology and the underlying mechanisms are unclear. In this paper, we describe the discovery of an unexpected beneficial role of muropeptides in regulating host mitochondria (Mt) homeostasis, development and food behavior, as well as the underlying mechanism.

Results

Bacterial PG metabolites support development and food behavior in *C. elegans*

To search for beneficial impacts of individual bacterial metabolites on animals, our lab has performed genetic screens of the Keio collection of *E. coli* (Baba et al., 2006) for developmental and behavior defects in *C. elegans* using multiple assay conditions (Qi and Han, 2018). After identifying a PG-related mutant during a pilot screen using an established assay (Govindan et al., 2015), we assembled and screened a sub-library that contains 57 PG metabolism mutants (Table S1). We found that worms fed 4 mutant bacterial strains (called PG mutants thereafter) displayed significantly developmental delay (Figures 1A, 1B and Figure S1E). Two of these mutants (*erfK* and *ycbB*) were also among candidates from an independent screen of the Keio collection for developmental delay (Zhang et al., 2019).

Previous studies from our lab and others have linked developmental delay to food avoidance (or lack of food dwelling) behaviors (Artyukhin et al., 2015; Brandt and Ringstad, 2015; Kniazeva et al., 2015; Liu et al., 2014; Melo and Ruvkun, 2012; Qi et al., 2017; Shtonda and Avery, 2006). We thus carried out a simply assay (Kniazeva et al., 2015) and found that feeding each of the PG mutants to *C. elegans* also trigger food avoidance behavior (Figures 1C and S1A). These data suggest that proper PG metabolism in *E. coli* have significant effects on host physiology.

Both the developmental delay and food avoidance behavior can be caused by either the presence of toxic molecules or the absence of beneficial metabolites (e.g., (Meisel et al., 2014; Melo and Ruvkun, 2012); Qi et al., 2017). One effective way to distinguish between these possibilities is to supplement the PG mutant with PG molecules isolated from wild-type *E. coli* and examine a potential rescue effect. We first supplemented heat-killed wild type (HK-WT) *E. coli*, which contains PG molecules, to worms fed live PG mutant *E. coli*, and found that the developmental delay and food avoidance behavior were almost completely overcome (Figures 1D-1F). We then isolated PG from wild type bacteria following two published protocols (Alvarez et al., 2020; Kuhner et al., 2014), and found that PG molecules isolated by each method were highly effective in overcoming the developmental delay and food avoidance phenotypes (Figures 1D-1F; Figures S1B and 1C).

To determine if the causes of the negative effects from feeding all 4 PG mutant *E. coli* are related, we fed animal with the mixture of two PG mutants of equal amounts. We observed that these double mutant *E. coli* mixtures induced growth delay at similar levels as single mutant *E. coli* feeding (Figure S1D). Together, the above results suggest that lack of common PG-related molecules in these PG mutants cause the defects in host animals, which is supported by further assays described below.

Deficiency in beneficial PG metabolites induces Mt stress in *C. elegans*

Cellular stresses and unfolded protein responses (UPR) are induced by environmental factors including bacterial metabolites (Frakes and Dillin, 2017; Grootjans et al., 2016; Kitamura, 2013; Labbadia and Morimoto, 2015; Mitra and Ryoo, 2019; Shpilka and Haynes, 2018). These stresses are known to play roles in animal development and food behaviors (Liu et al., 2014; Melo and Ruvkun, 2012). We examined the levels of several commonly used stress reporters (Taylor et al., 2014) in worms fed with these PG mutant *E. coli*, and found that Mt stress (P*hsp-6::gfp* and P*hsp-60::gfp*), but not ER stress (P*hsp-4::gfp*) nor cytoplasmic stress (P*hsp-16.2::gfp*), were strongly induced (Figures 2A-2C, 2E and 2F). Further support of Mt stress induction came from analysis of DVE-1, a critical co-factor in ATFS-1 mediated UPR^{mt} that is translocated into the nucleus upon Mt stress (Anderson and Haynes, 2020). We found that PG mutants feeding also promoted nuclear accumulation of DVE-1::GFP in the intestinal cells (Figures 2A and 2D). Importantly, we found that PG molecules isolated from wild-type *E. coli* also effectively suppressed Mt stress in *C. elegans* fed with each of the 4 PG mutants (Figure 2G). In addition, feeding worms with a mixture of two PG mutants induced UPR^{mt} at similar levels as feeding with single mutants (Figure S2A). These data also support that these PG mutants lack common, beneficial PG-related molecules. We also performed additional tests to show that the observed developmental defects of worms fed with these PG mutants are not likely due to iron deficiency or innate immune response through the PMK-1/p38 or a p38 independent pathway in *C. elegans* (Figures S2B-S2F) (Bolz et al., 2010; Dunbar et al., 2012; Girardin et al., 2003a; Gottar et al., 2002; Irazoki et al., 2019; Royet et al., 2011; Zhang et al., 2019).

The beneficial role of PG in *C. elegans* is not an indirect effect on bacterial physiology

We next carried out three sets of experiments to determine if the beneficial effect of PG on the host is due to an indirect effect on *E. coli* physiology. First, we mixed wild-type and

mutant bacteria in several different ratios and fed each mix to *C. elegans*. We observed that the 1:4 ratio fully rescued the functions in *C. elegans* (Figure S3A and S3B), suggesting that the observed defects in *C. elegans* fed PG mutant *E. coli* is unlikely due to potential slower growth of the mutant bacteria. In the second experiment, we employed an assay where L1 larvae are placed on a plate with a large quantity of heat-killed bacteria (150 μl) and a tiny amount of live bacteria (0.2 μl) spotted in separate locations (Qi and Han, 2018). Worms can use heat-killed bacteria as food to support growth if they first ingest a small amount of live bacteria (Qi and Han, 2018). We found that, compared to worms fed heat-killed wild-type *E. coli*, worms fed heat-killed PG mutant bacteria displayed growth delay and mitochondrial stress (Figure S3C and S3D). These results support that the benefits of PG are unlikely due to an indirect impact on bacterial physiology. Finally, we generated a germ-free food condition to obtain more conclusive evidence on this issue. In a previous study, we showed that worms fed heat-killed bacteria are able to proceed through postembryonic growth (albeit at a slower pace) if certain vitamins are added (Qi et al., 2017). Following this idea, we mixed a synthetic medium (*C. elegans* maintenance medium or CeMM) (Zhang et al., 2015) with heat-killed bacteria and observed a significant difference between the ability of heat-killed wild-type bacteria and heat-killed mutant bacteria to support animal growth and suppress mitochondrial stress (Figure 2H, 2I and Figure S3E-S3H). Moreover, adding isolated PG or anti-oxidant NAC to the food effectively suppressed the defects under the germ-free condition (Figure 2H, 2I and Figure S3E -S3I). These results strongly support that at least the majority of the beneficial roles of PG in *C. elegans* are not through an indirect effect on bacterial physiology.

The beneficial role of PG is largely mediated by suppression of Mt oxidative stress

Mt are the major endogenous source of reactive oxygen species (ROS), especially under stress conditions (Dingley et al., 2010; Lee et al., 2010). The *sod-3* gene, encoding a Mt manganese superoxide dismutase, is a known oxidative stress response gene (Libina et al., 2003). Using a SOD-3::GFP reporter, we observed a significantly increased level of SOD-3 expression in *C. elegans* fed *erfK* mutant *E. coli* compared to control (Figure 2H). Importantly, the increase in SOD-3 level was eliminated by adding isolated PG or antioxidant NAC (N-acetyl-L-cysteine) (Figure 2H), which was also confirmed by a ROS staining assay (Figure S2G), indicating a role of the beneficial PG molecules in suppressing ROS production in Mt. Moreover, we found supplementation of antioxidant NAC significantly suppressed the developmental delay, food avoidance and Mt stress induced by feeding worms with PG mutant *E. coli* (Figures 2K-2M and S3J), supporting the idea that suppressing Mt oxidative stress is critically involved in the protective role of the PG molecules. To exclude the indirect effect of NAC or PG on live mutant bacteria to suppress ROS, we supplemented NAC or PG and HK bacteria to worms under the germ-free food condition (CeMM plates). We found that both NAC and PG supplementation decreased ROS production in *C. elegans* (Figure S3I), supporting that NAC and PG benefit the host directly to suppress Mt oxidative stress.

Beneficial muropeptides contain disaccharides with short peptides

To learn more about the structural properties of the beneficial PG molecules, we employed several enzymes, including those that cleave PG at specific sites (Figure 3A). We first treated

PG with Proteinase-K, which is a broad-spectrum protease (Kraus and Femfert, 1976), and found that the rescue effect of PG was abolished (Figures 3B-3D, ProK-PG). In contrast, treatment with trypsin, a serine protease used in the final step of the PG isolation protocol (Figure S4A), preserved the rescue effect (Figures 3B-3D, control-PG). We then treated the PG with Amidase (AmiD) that cleaves the short amino acid peptides from PG (Figure 3A) and found that the rescue effect of PG was eliminated (Figures 3B-3D, AmiD-PG). These results suggest that the proposed beneficial molecules do not contain lipoproteins known to attach to PG (trypsin sensitive), whereas the attachment of the short amino acid peptides to PG molecules (Proteinase-K sensitive, Amidase-sensitive, but trypsin insensitive) are needed for the beneficial effect.

We then further examined the structure of the beneficial PG molecule by treating the active PG mix with lysozyme that cuts the bond between the 5' *N*-acetylmuramic acid (NAM) and 3' *N*-acetylglucosamine (NAG) or N-acetyl-glucosaminisase (NagZ) that cuts the bond between the 5'NAG and 3'NAM (Figure 3A)(Irazoki et al., 2019). Either treatment is expected to generate disaccharide-peptide molecules (disaccharide containing muropeptides). While the lysozyme treatment did not significantly affect the role of PG mix in suppressing Mt stress and growth delay in *C. elegans* fed *erfK* mutant *E. coli*, the NagZ treatment effectively eliminated such a suppression role (Figures 3B-3D, lysozyme-PG and NagZ-PG). To further confirm the efficiency of the muropeptides, we collected the supernatant from lysozyme treated PG and found that the muropeptides in the supernatant are sufficient to suppress the host phenotypes (Figures 3E-3G). These results suggest that the effective PG molecules are likely 5'NAG-NAM disaccharide muropeptides with an amino acid peptide attached to NAM. Further analyses using mixtures of products of specific PG purification steps from the mutants support that certain PG hydrolysis activities including removal of lipoproteins attached to PG are involved in releasing the beneficial PG muropeptides (Figures S4A-S4D).

Muropeptides accumulate in intestinal Mt

Since feeding PG mutant diet specifically induced Mt stress, we asked whether muropeptides accumulate and function in Mt to support host functions. We thus employed an established method to label PG with fluorescein isothiocyanate isomer I (FITC) (Mann et al., 2016) and then examined PG muropeptide distribution in *C. elegans*. We first showed that the FITC-labeled PG (FITC-PG) is functional, as it suppresses the developmental delay phenotype in worms fed the *erfK E. coli* (Figure 4A). Microscopy of animals fed with MitoTracker dye and FITC-PG revealed strong FITC-muropeptide signals in the intestinal cells (Figure 4B and 4C) and FITC-PG puncta in intestinal lumen (Figure S5). We then isolated Mt from FITC-PG fed animals and found that 34% of isolated Mt were labeled with both FITC-muropeptides and MitoTracker dye (Figure 4D), which further supports that muropeptides reside in Mt. FITC negative Mt (66%) were likely isolated from non-intestinal tissues that may not absorb FITC-muropeptides (Figure 4D).

We further examined the muropeptide level in worm Mt by employing an established HEK-Blue-NOD1 assay (InvivoGen)(Packiam et al., 2015). In this assay, HEK293 cells were transformed with genes encoding the muropeptide receptor NOD1 and the NF-κB SEAP

reporter. Muropeptides added to the culture will bind to NOD1 and activate the expression of the downstream NF-κB SEAP reporter, leading to a change in medium color. Here we found that Mt lysates from worms induced NOD1 activity (Figure 4E), providing further evidence that muropeptides accumulate in *C. elegans* Mt. In addition, the activity in the Mt lysates from worms fed wild-type *E. coli* was significantly higher than that from worms fed *erfK E. coli* (Figure 4E), indicating that the Mt accumulation of muropeptides is significantly reduced in *C. elegans* fed the mutant *E. coli*.

Muropeptides interact with ATP synthase for the beneficial functions

To gain more insight into the mechanism underlying the beneficial effects of muropeptides on host animals, we performed PG pull down and mass spectrometric (MS) analysis to identify PG-binding proteins (Baik et al., 2015) in *C. elegans*. Using a relatively stringent cut-off point of score at 35, we identified 168 peptides as potential protein interactors with PG (Table S2). If the interaction of PG molecules with a particular protein is critically involved in the beneficial impact of the muropeptides on animal physiology, then RNAi knockdown of the candidate may generate phenotypes similar to that caused by the PG mutant diet. We thus performed RNAi analysis of all 168 candidate genes and found RNAi of 6 of them, including 5 that encode Mt proteins, significantly increased P*hsp-6::gfp* expression, developmental delay and food avoidance behavior (Figures 5A-5D, S6A and S6B). Interestingly, 4 of these 5 Mt proteins are subunits of the F1 complex of ATP synthase (*atp-1, atp-2, atp-4, atp-5*) (Figure S6A).

We then carried out three additional tests to analyze the interaction between PG muropeptides and ATP synthase. First, we incubated isolated PG from wild-type *E. coli* with worm lysate and found that the PG molecules efficiently bound to ATP-1 in a concentration dependent manner (Figure 5E). Second, we treated PG with Proteinase-K and found that Proteinase-K treated PG can no longer pulldown ATP synthase (Figure 5F), which suggests that the short amino acid peptides associated with muropeptides are necessary not only for the functions, as shown earlier (Figures 3B-3D, ProK-PG), but also for binding to ATP synthase. Finally, we found that the step 3 product of PG purification (prior to trypsin treatment) failed to pull down ATP-1 (Figure 5G), consistent with the notion that presence of lipoprotein compromises the effect of muropeptides (Figures S4B-S4D, *erfK* and *ygeR*). Collectively, these results indicate that the ability of PG muropeptides to bind ATP synthase is tightly correlated with the ability to provide the beneficial function in *C. elegans*.

We further tested whether the ATP synthase impacts muropeptides distribution and function. Since *atp-1(RNAi)* causes first generation developmental arrest and F1 cannot be tested, we knocked down *atp-4*, which partially induces the phenotypes in the F1 generation. First, we showed that knockdown of *atp-4* significantly reduced the level of intestinal FITC-muropeptides (Figure 5H), indicating that ATP-4/ATP synthase is necessary for the accumulation of muropeptides in the intestine. Second, while adding isolated PG to worms fed *erfK E. coli* could suppress the phenotypes (Mt stress, developmental delay and food avoidance), this suppression effect was eliminated when the PG was added to *atp-4(RNAi)*-treated worms (Figures 5I-5K). Together, these data revealed a mechanism by which the

muropeptides-ATP synthase interaction plays a critical role in mediating the beneficial effect of PG on the host physiology.

Muropeptides display antagonistic interaction with a known ATP synthase inhibitor

Previous studies have shown the profound impact of inhibiting ATP synthase activity on Mt ROS production, cellular metabolism, aging and cancer cell progression (Alavian et al., 2011; Chin et al., 2014; Esparza-Molto and Cuezva, 2018; Goldberg et al., 2018). The ATPase Inhibitory Factor 1 (IF1) is a known physiological inhibitor of ATP synthase that acts through binding to the F1 domain of the enzyme, and has been shown to play important roles in both mammalian cells and *C. elegans* under stress conditions and in tumor cells (Bason et al., 2014; Campanella et al., 2008; Garcia-Aguilar and Cuezva, 2018; Garcia-Bermudez et al., 2015; Pullman and Monroy, 1963). The *C. elegans* genome encodes two IF1 homologs, MAI-1 and MAI-2 (Ichikawa et al., 2006), but only MAI-2 contains the Mt targeting sequence (MTS) (Fernandez-Cardenas et al., 2017). We thus tested the functional relationship between muropeptides and MAI-2 by measuring the growth rate, UPR^{mt} and food avoidance behavior in a *mai-2* loss-of-function *(−)* mutant, *mai-2(xm19)* (Fernandez-Cardenas et al., 2017). Indeed, *mai-2(−)* partially alleviated all the phenotypes in worms fed *erfK* mutant *E. coli* (Figures 5L-5N and S6C and S6D). In addition, RNAi analysis confirmed that *mai-1* is not critically involved in the process (Figure S6E). This antagonistic relationship between muropeptides and a known inhibitor of ATP synthase provides further support for the role of muropeptides as an ATP synthase agonist.

Discussion

This study uncovered a previously unknown beneficial or nutritional role of bacterial muropeptides in regulating host physiology and insights of the underlying mechanism (Figure 6). We provide evidence that *E. coli* muropeptides act to promote *C. elegans* post-embryonic development and food dwelling behavior and do so at least in part by entering the Mt of intestinal cells and binding to ATP synthase. Our data also suggest that the changes in oxidative stress and UPR^{mt} are largely responsible for the PG muropeptide-related phenotype changes in postembryonic development and food behaviors in *C. elegans*. Given the abundant presence of commensal gut bacteria across the animal kingdom including in humans and exceptional structural conservation of ATP synthase, the beneficial usage of the bacterial muropeptides by the host is likely conserved in mammals. Therefore, our study may have uncovered an unexpected beneficial role of an individual bacterial metabolite and the fascinating underlying mechanism, which also provides valuable insights into the symbiotic relationship between the host animals and commensal microbes and adds to the evidence that the Mt is an important hub for host-microbiome interaction.

Previous studies have identified numerous protein and chemical inhibitors of ATP synthase and shown the profound impact of the inhibition on Mt ROS production, cellular metabolism, aging and cancer cell progression (Alavian et al., 2011; Chin et al., 2014; Esparza-Molto and Cuezva, 2018; Goldberg et al., 2018; Hong and Pedersen, 2008). However, since essentially no ATP synthase agonists have been previously described, our study may have uncovered such an ATP synthase agonist and shown that this agonist

is normally present in animal intestine cells to execute such a role. This interaction between PG muropeptides and ATP synthase may be a powerful tool to address a variety questions regarding Mt homeostasis, energy balance and disease conditions in different model systems.

The isolated PG are large molecules that are not likely absorbed directly by the host cells. Indeed, in the FITC-PG feeding assay, we only observed PG puncta (large molecules) in intestinal lumen but not inside of Mt or cells of the intestine (Figures 4B, 4D and S5). This observation is consistent with our model that the functional molecules are muropeptides that are the breakdown products from PG. This conclusion is based on our functional assays showing that muropeptides from lysozyme-treated PG are sufficient to suppress Mt stress, developmental delay and food avoidance caused by feeding PG defective bacteria to *C. elegans* (Figures 3E-3G). In the intestine, PG may be broken down into muropeptides by the combination of two processes. First, large PG molecules may be hydrolyzed by enzymes produced by the host animals. Animal genomes contain a number of lysozyme genes (e.g., *lys-1-10* and *ilys-1-6* in *C. elegans*), and some are expressed constitutively in the intestine to digest PG (Schulenburg and Boehnisch, 2008). Second, during bacterial proliferation, partial degraded PG molecules are released into the environment (Goodell and Schwarz, 1985; Park and Uehara, 2008). As indicated by the defects of the 4 PG mutant *E. coli*, activities of certain PG metabolic enzymes are required to generate PG molecules that can be further processed to produce functional muropeptides.

In this study, we focused on intestinal cells for obvious reasons, but PG muropeptides derived from commensal bacteria may also enter other cell types to impact host physiology. In mammals, a previous study indicated that muropeptides can even enter the nervous system (Arentsen et al., 2018). Given that the intestine has abundant commensal bacteria, it is conceivable that the observed effects of PG muropeptides on mitochondrial functions is weaker in other tissues. In addition, energy production from mitochondria varies from tissue to tissue and the need or effect of factors to boost or inhibit ETC and ATP synthase may vary. For example, IF1 is a well-known protein inhibitor of ATP synthase, and its expression level in different mammalian cells varies widely (Garcia-Aguilar and Cuezva, 2018). The combination of muropeptides and MAI-2 (IF1 ortholog) may provide a way for worms to regulate Mt homeostasis under different conditions.

Besides ATP synthase subunits, the combination of PG pull-down assay and RNAi analysis identified another Mt protein UCR-1, which is a complex III subunit of electron transport chain (Figures 5A-5D and S6A and S6B). This interaction may suggest that the muropeptides can positively influence Mt oxidative respiration through interaction with multiple components of the electron transport chain, whose activity is dynamically regulated to meet cellular metabolic status (Lapuente-Brun et al., 2013).

In this study, we identified four genes from testing mutants of 57 PG-related genes; feeding worms with the *E. coli* mutants of these four genes led to prominent developmental defects. The small number of genes may be close to what should be expected based on the structural property of the muropeptide uncovered by our enzymatic analysis. First, the active PG molecules appear to be free of lipoprotein, and this state appears to be required, as the

trypsin treatment preserves the activity. Second, two of the four enzymes might be involved in separating linkages between AA peptides from parallel rows of PG (*dacB* and *ycbB*), albeit that the exact enzymatic activities are not necessarily clear. Third, the larger PG fragment may be processed to disaccharide by lysozymes produced by the *C. elegans* intestine as mentioned above, and many other known hydrolysis enzymes are not expected to be required. For example, one would not expect any of the 5 amidases to be required because the attached AA peptide is needed based on our data from proteinase K or amidase treatment. Similarly, enzymes involved in the attachment of PG to lipoprotein (Ldt enzymes other than *erfK*) are also not expected to be required. Based on structural similarity, *erfK* (aka LdtA) is a Ldt family protein known to facilitate the attachment of lipoprotein to PG (Magnet et al., 2007). However, unlike LdtB, erfK/LdtA is not the main enzyme to catalyze the function ((Magnet et al., 2007; Sanders and Pavelka, 2013), which may open the possibility for a potential opposite role associated with *erfK*: detaching PG from lipoprotein. Such a speculation seems to be supported by the tests presented in Figure S4, where PG isolated from *erfK* mutant bacteria can still rescue the Mt stress and developmental defects in worms, as long as the PG isolates are treated with trypsin. Since WT PG isolates can rescue without the trypsin treatment, the *erfK* enzyme has the same effect on PG from WT bacteria as trypsin does on *erfK* mutant. Therefore, this result may suggest that an altered interaction between certain lipoproteins and PG may prevent the release of functional muropeptides from the mutant bacteria or isolated PG without trypsin treatment. *ygeR* is suggested to encode a putative PG hydrolase based on the presence of a LytM (lysostaphin)-Domain, but the exactly function is still unknown(Typas et al., 2011; Uehara et al., 2009).

Limitations of the study

It is possible that our screen and subsequent tests have missed a small number of enzymes required for producing the active PG fragments due to either lethality associated with the bacterial mutation or due to genetic redundancy. Regarding possible redundancy, there is no clear-cut enzyme class with good rationale underlying the potential miss by the screen. It might be important to mention that the exact enzymatic functions of many *E. coli* PG-related enzymes are yet to be determined by biochemical methods. In addition, it is important to note that the exact enzymatic functions of many *E. coli* PG-related enzymes are yet to be determined by biochemical methods, which was not addressed in this study.

Our structural analyses based on enzymatic effects of isolated PG in functional assays have led to the prediction that the beneficial PG molecules are likely 5’NAG-NAM disaccharide muropeptides with an amino acid peptide attached to NAM. However, such a prediction needs to be confirmed by further separation methods coupled with functional assays and subsequent structural analysis using mass spectrometry, which is needed to determine the composition of the effective peptides.

In this study, we made a significant effort, including using a feeding condition without live bacteria, to provide evidence that the major beneficial effect of isolated PG is not an indirect effect on bacterial physiology. We need to point out that these tests were not designed to exclude the potential effects of isolated PG on bacterial functions. In addition, the conclusion of a direct impact of PG muropeptides on functions in animal cells would

be further confirmed by testing the role in cultured cells under a completely germ-free condition, which is being carried out in our lab.

Finally, although our data has led to the model that the beneficial PG muropeptides enter mitochondria of animal cells and execute the impacts through binding to ATP synthase, the model may not be firmly established until we learn more about the mechanistic detail. Structural analysis of the interaction between the muropeptides and ATP synthase, including identifying the specific subunit that binds to the muropeptides and the potential impact of the binding on the structural/functional properties of the large enzyme, would be highly desirable.

STAR METHODS

RESOURCE AVAILABILITY

Lead contact—Further information and requests for reagents should be directed to the Lead contact Min Han (mhan@colorado.edu).

Materials availability—Unique and stable reagents generated in this study are available from the Lead contact with a completed Materials Transfer Agreement.

Data and code availability

- Original western blot images and microscopy data reported in this paper will be shared by the lead contact upon request.
- This paper does not report original code.
- Any additional information required to reanalyze the data reported in this paper is available from the lead contact upon request.

EXPERIMENTAL MODEL AND SUBJECT DETAILS

C. elegans* strains and maintenance—C. elegans* strains were grown and maintained on nematode growth media (NGM) plates seeded with the *Escherichia coli* strain OP50 at 20 °C(Brenner, 1974). The following strains were obtained from *Caenorhaditis* Genetics Center (CGC): N2 Bristol (wild-type control strain), SJ4100: *zcIs13[*P*hsp-6::gfp]* V, SJ4058: *zcIs9[*P*hsp-60::gfp + lin-15(+)]* V, SJ4197: *zcIs39[*P*dve-1::dve-1::gfp]* II, SJ4005: *zcIs4 [*P*hsp-4::gfp]* V, TJ375: *gpIs1 [*P*hsp-16.2::gfp],* AY101: *acIs101 [*P*F35E12.5::gfp + rol-6(su1006)],* AU133: *agIs17 [*P*myo-2::mCherry + Pirg-1::gfp]* IV, CF1553: *muIs84 [(pAD76) sod-3p::GFP + rol-6(su1006)]. mai-2(xm19)* was obtained from Dr. R. E. Navarro (Universidad Nacional Autonoma de Mexico).

METHOD DETAILS

***E. coli* Keio collection screen—**Bacterial peptidoglycan (PG) metabolism-related genes were determined based on the published papers(Juan et al., 2018; Typas et al., 2011; van Heijenoort, 2011; Vollmer and Holtje, 2004) (Table S1) and the PG mutant sub-library was assembled from the Keio *E. coli* single mutant collection(Baba et al., 2006). Mutant bacteria strains, as well as the wild-type control strain BW25113, were cultured overnight in LB

medium with 50 μg/ml kanamycin in 96-well plates at 37 °C. 100 μl of the overnight *E. coli* cultures were spotted onto 6 cm NGM plates and dried at room temperature for 1h before use. About 200 synchronized L1 worms were then placed on the seeded NGM plates and cultured at 20 °C. Animals were screened after 54-56 hours. Worm developmental rates were determined by vulval development as previously described(MacNeil et al., 2013). To quantify the developmental rate, about 50 animals were scored under Nomarski microscope.

To verify the genotypes of the 4 candidate Keio mutants, PCR were performed on each mutant colony and the control BW25113 strain using specific downstream genomic primers together with kanamycin-cassette-specific primers (Oligonucleotides in STAR METHOD) (Baba et al., 2006) (Figure S1C).

Food avoidance behavior assay—Food avoidance behavior assay was determined using a method adapted from a published procedure(Kniazeva et al., 2015; Melo and Ruvkun, 2012). Briefly, overnight cultures of wild type and PG mutant *E. coli* were adjusted to the same OD_{600} and 20 μl of each culture was seeded on the center of 6 cm NGM plates. The seeded plates were dried at room temperature for 1 hour before use. About 100 synchronized L1 animals were then dropped onto the bacterial lawns and cultured for 45 hours at 20 °C. The avoidance index was determined by $N_{off/on}/N_{total}$. Each assay was conducted in triplicate.

Heat-killed *E. coli* preparation and supplementation—We followed an established protocol(Qi et al., 2017) to prepare heat-killed (HK) *E. coli*: standard overnight bacterial cultures were concentrated to 1/10 vol and were then heated in a 75 °C water bath for 90 min. For HK-*E. coli* supplementation, live *E. coli* and HK-*E. coli* were mixed at a 1:1 ratio then 20 μl (avoidance behavior assay) or 50 μl (other assays) mixtures were dropped on the NGM plates and dried at room temperature for 10 min before use. About 100-200 synchronized L1 animals were placed on the bacterial lawn to grow at 20 °C.

PG isolation, enzyme treatment and supplementation assays—Two established methods were used to isolate peptidoglycan from bacterial cultures. In brief, following the first method (Kuhner et al., 2014), bacterial pellets were resuspended in 1/10 vol 1M NaCl solution and boiled at 100 °C in a heating block for 1h. After washing 4 times with distilled water, the insoluble cell wall preparations were incubated in an ultrasonic water bath (Laboratory Supplies Co., INC, G112SP1T) for 1h, followed by stepwise digestion using DNAse/RNAse and trypsin at 37 °C for 1h, respectively. The solutions were boiled for 5 min at 100 °C to inactive the enzymes, followed by washing twice with distilled water. The PG pellets were recovered by centrifugation at 13,000 rpm for 10 min and stored at 4 °C. In the second method (Alvarez et al., 2020), the bacterial pellets were boiled in SDS solution to solubilize all cell components except for PG. All the soluble components and SDS were then removed by ultracentrifugation (150,000 x *g*) for several times, and the lipoproteins on PG were digested by trypsin at 37 °C for 1h. The solutions were boiled for 5 min at 100 °C to inactive the enzymes, followed by washing twice with distilled water.

For further enzymatic treatment of isolated PG, lysozyme (Fisher 44-031-GM, 300 μg/ml), AmiD (purified from BL21 *E. coli*, 300 μg/ml) or NagZ (purified from BL21 *E. coli*, 300

μg/ml) were added to PG solution (20 mM HEPES pH7.5) and incubated at 37 °C for 48h. The enzymatic reactions were stopped by incubating with 50 μg/ml trypsin at 37 °C for 2h. The supernatants were collected after centrifugation at 12,000 rpm for 10min. Muropeptides were collected from the supernatant of lysozyme-treated PG and stored at −20 °C for further assays. For proteinase K treatment, 400 μg/ml proteinase K was added to PG solution (20 mM HEPES pH7.5) and incubated at 37 °C for 2h. The enzymatic reaction was stopped by boiling at 100 °C for 15 min.

For supplementation assays, indicated volume of live *E. coli* and PG solution mixtures (1:1 ratio) were seeded on NGM plates and dried for 10 min. *C. elegans* feeding assays were performed as described above.

Mixed *E. coli* feeding assays—Overnight *E. coli* cultures were adjusted by OD_{600}. WT and PG mutant cultures were mixed to different ratios as described in figure legends and spotted on NGM plates and dried for 10 min at room temperature. About 100 synchronized L1 animals were then placed on the bacterial lawn to grow at 20 °C.

Assay using heat-killed bacteria and CeMM medium—CeMM medium (Table S3) was made following a published recipe (Zhang et al., 2015). Briefly, all the chemical components were dissolved in distilled water and filtered through a 0.25μm filter. The liquid CeMM medium was spotted on NGM plates and dried at room temperature, then 100 μl of heat-killed *E. coli* was added to each plate. About 200 synchronized L1 animals were seeded on the CeMM plates to grow at 20 °C.

Assay using the combination of live bacteria and heat-killed bacteria.—In a previous established assay (Qi and Han, 2018), *C. elegans* were shown to be able use heat-killed *E. coli* as the main food only if they also took a tiny amount of live *E. coli* to colonize their gut. The procedure was adopted in this study to test the difference between heat-killed wild-type and heat-killed mutant *E. coli*. In brief, 0.2 μL of overnight bacterial culture were seeded on one side of NGM plates. 150ul heat-killed (HK) bacteria, which were prepared as described above, were placed on the other side of the NGM plates. Then, about 300 synchronized L1 worms were added to the side of the plates with live bacteria and cultured at 20 °C.

Chemical supplementation—The NAC (Fisher Scientific, ICN10009825) stock solution (500 mM) was made in ddH2O. For NAC supplementation, NAC solution was added in NGM agar to the final concentration of 50 mM. For iron supplementation, $FeCl_3$ (Sigma, 236489) was dissolved in ddH2O to generate solutions of desired concentration (2 mM, 8 mM and 20 mM). The $FeCl_3$ solutions were mixed with live *E. coli* (1:1 ratio) and seeded on the NGM plates.

For tunicamycin treatment, tunicamycin (Fisher Scientific, ICN15002801) was mixed with live *E. coli* to a final concentration of 5 βg/ml and spotted on the NGM plates.

C. elegans feeding assays were performed as described above.

Heat shock treatment of worms—100 synchronized L1 larvae were grown to early L4 (24 h, 20 °C), then incubated at 35 °C for 1 h and allowed to recover overnight at 20 °C before microscopic examination.

FITC-PG labeling—An established protocol was modified to label PG with FITC(Mann et al., 2016). Briefly, PG was isolated as described above and then sonicated in a water-bath sonicator for 1 h. The sonicated PG was suspended in 500 μl FITC solution (Fisher, 71-190-0, 1mg/ml in sterile carbonate buffer). The tubes containing the solutions were wrapped in aluminum foil to avoid exposure to light and shaken for 1h at room temperature. The FITC-PG sample was washed more than 6 times to remove unlabeled FITC and resuspend in ddH2O. The FITC-PG feeding assays were performed as described in PG supplementation procedures. As negative controls, 10 μM MitoTracker-Red CMXRos and/or FITC dye were supplemented on live bacteria lawns. All the NGM plates were wrapped in aluminum foil to protect from light. L4 larvae animals were fixed in 4% formaldehyde with 6 mM K_2HPO4 (PH 7.2) and 75% methanol for 10 min at −20 °C to remove auto-fluorescence in the intestine. The fixed worms were rinsed three times in PBS before microscopic examination.

Mitochondrial (Mt) extraction—Mt from worms were extracted from L4 larvae with the Mt Isolation Kit for Tissue (Thermo Scientific, 89801), following the manufacturer's protocols.

HEK-Blue –NOD1 assay—Isolated Mt were lysed with Tris-buffed saline (25 mM Tris-Hcl, pH 7.2, 150 mM NaCl, 1x protease inhibitor) and centrifuged at 12,000g for 5 min to collect the supernatant. Samples were adjusted based on Mt total protein as determined by the BCA protein assay kit (Thermo Scientific, 23225). HEK293 cells expressing the human NOD1 receptor and the NF-κB SEAP reporter genes (Invitrogen, hkb-hnod1) were used according to the manufacturer's instructions to assess the muropeptides in mitochondrial lysates. In brief, 20 μL of adjusted Mt lysates, or lysis buffer (mock), were added to single well of a 96-well plate. A cell suspension (~280,000 cells per ml in HEK Blue detection medium) was prepared and 180 μl was added to wells with mitochondrial lysates or mock lysate. The 96-well plate was incubated at 37 °C overnight and assessed by reading OD at 650 nm.

Isolation and identification of PG binding proteins—A modified method was used to identify the PG binding proteins from *C. elegans* lysate(Baik et al., 2015). In brief, ~100 μl worm pellet was suspended in lysis buffer (100 mM NaCl, 0.5mM EDTA, 0.5% NP-40 and a cocktail of protease inhibitors in 10 mM Tris-HCl, pH 7.4), followed by sonication. After centrifugation, the supernatant was mixed with about 200 μg isolated PG and incubated at 4 °C for 1 h. The PG binding proteins (PG-BPs) were collected by centrifuging at 4 °C at 13,000 g for 10 min. After washing 3 times with a wash buffer (150 mM NaCl in 10 mM Tris-HCl, pH 7.4), proteins that bound to PG were eluted by boiling at 100 °C for 15 min. The supernatant was collected by centrifuging at 13,000 g for 10 min and subjected to LC-MS analysis.

Protein expression and purification—The nagZ (1-1023bp) and AmiD (52-831bp) genes were PCR amplified from WT K-12 BW25113 genomic DNA. All gene constructs were inserted into a pET28a vector. These constructs were transformed into *E. coli* BL21(DE3) cells and grown in LB broth at 37 °C overnight. The overnight cultures were diluted with 1/100 vol of fresh LB broth and cultured until OD_{600} reached ~ 0.6. The expression of recombinant proteins was induced by 0.1 mM IPTG at 20 °C for 19 h. Bacterial cells were harvested by centrifugation at 5000 g for 10 min at 4 °C. After centrifugation, the pellets were lysed in buffer containing 25 mM HEPES pH 7.5, 500 mM NaCl, 0.5% NP-40, 1 mM DTT and 1x protease inhibitor, followed by centrifugation at 12,000 g for 30 min at 4 °C. The supernatants were incubated with Ni-NTA agarose beads (Qiagen, 151028822) for 1 h and rinsed 3 times with a wash buffer (25 mM HEPES pH 7.5, 500 mM NaCl, 1 mM DTT and 30 mM imidazole). Proteins were eluted with buffer containing 25 mM HEPES pH 7.5, 500 mM NaCl, 1mM DTT and 500 mM imidazole. Amicon Ultra centrifugal filters (10kD) were used to concentrate the proteins and exchange buffer (25 mM HEPES pH 7.5, 250 mM NaCl and 1 mM DTT). These proteins were then stored at −80 °C with 10% glycerol.

Verification of the interaction between PG and ATP synthase α-subunit—To confirm the interaction between PG and ATP-1 (*C. elegans*) or ATP5A1(mammals), PG pull-down assays were performed as described above. Total protein of worms or caco-2 cell lysates were used to incubate with PG, proteinase K treated PG or PG3. PG. Western blots were performed to detect ATP-1 (*C. elegans*) or ATP5A1 (caco-2 cells) (Thermo Fisher 43-9800)(Qi and Han, 2018).

RNAi treatment in *C. elegans*—RNAi plates were prepared by adding IPTG to NGM agar to a final concentration of 1 mM. Overnight *E. coli* cultures (LB broth containing 100 μg/ml ampicillin) of specific RNAi strains and the control HT115 strain were seeded to RNAi feeding plates and cultured at room temperature for 2 days before use. Synchronized L1 animals were added to the RNAi *E. coli* seeded plates. For transgenerational RNAi knockdown of *atp-4*, we fed synchronized L1 animals with OP50 for the first 12 h and then transferred the worms to *atp-4* RNAi or control plates. The gravid adults were bleached to collect synchronized F1 worms, which were then fed with PG mutant *E. coli*.

ROS measurements in *C. elegans*—The ROS staining protocol was modified from (Coppa et al., 2020). Briefly, L4 stage animals were collected and washed three times with M9 buffer to remove the bacteria. Then the worms were transferred into the staining solution (H2DCFDA, 50 uM in M9 buffer) and incubated for 30 min at 20°C. After washing twice with M9 buffer, worms were subjected to microscopic examination.

Microscopy—Analysis of fluorescence was performed under Nomarski optics on a Zeisis Axioplan2 microscope with a Zeiss AxioCam MRm CCD camera. Plate phenotypes were observed using a Leica MZ16F dissecting microscope with a Hamamatsu C4742-95 CCD camera.

QUANTIFICATION AND STATISTICAL ANALYSIS

ImageJ software was used for quantifying fluorescence intensity of various of reporters. Late L4 to young adults were randomly picked under dissection microscope and imaged by the Nomarski microscope. To determine the developmental stages, animals were cultured 54-56 h, with the exception that animals for NAC supplementation and *mai-2(−)* were cultured about 60-62 h, before microscopic evaluation. We used the Student's t-test to determine the significant differences as indicated in the figure legends.

Supplementary Material

Refer to Web version on PubMed Central for supplementary material.

Acknowledgements

We thank Drs. Felipe Cava (Univ. of Umea), Jose Cuezva (Univ. of Autonoma de Madrid), Ute Bertsche (Univ. of Tübingen), Michael Stowell, James Orth, Thomas Lee and Ding Xue (Univ. of CO) and our lab members for providing helpful advice and discussion, Dr. Rosa Estela Navarro (Univ. Nacional Autonoma de Mexico) for sharing the *mai-2(−)* mutant, Mass Spectrometry Facility and Light Microscopy Facility at University of Colorado for facilitating the analyses, and Aileen Sewell for critical editing of the manuscript. Some strains were provided by the *Caenorhabditis* Genetics Center (supported by NIH P40 OD010440). This study was supported by NIH grant 5R01GM047869 (MH) and 1R35GM139631 (MH).

References

Alavian KN, Li H, Collis L, Bonanni L, Zeng L, Sacchetti S, Lazrove E, Nabili P, Flaherty B, Graham M, et al. (2011). Bcl-xL regulates metabolic efficiency of neurons through interaction with the mitochondrial F1FO ATP synthase. Nature cell biology 13, 1224–1233. [PubMed: 21926988]

Alvarez L, Cordier B, Van Teeffelen S, and Cava F (2020). Analysis of Gram-negative Bacteria Peptidoglycan by Ultra-performance Liquid Chromatography. Bio-protocol 10, e3780. [PubMed: 33659436]

Anderson NS, and Haynes CM (2020). Folding the Mitochondrial UPR into the Integrated Stress Response. Trends in cell biology 30, 428–439. [PubMed: 32413314]

Arentsen T, Khalid R, Qian Y, and Diaz Heijtz R (2018). Sex-dependent alterations in motor and anxiety-like behavior of aged bacterial peptidoglycan sensing molecule 2 knockout mice. Brain, behavior, and immunity 67, 345–354.

Artyukhin AB, Yim JJ, Cheong Cheong M, and Avery L (2015). Starvation-induced collective behavior in C. elegans. Scientific reports 5, 10647. [PubMed: 26013573]

Baba T, Ara T, Hasegawa M, Takai Y, Okumura Y, Baba M, Datsenko KA, Tomita M, Wanner BL, and Mori H (2006). Construction of Escherichia coli K-12 in-frame, single-gene knockout mutants: the Keio collection. Molecular systems biology 2, 2006 0008.

Baik JE, Jang YO, Kang SS, Cho K, Yun CH, and Han SH (2015). Differential profiles of gastrointestinal proteins interacting with peptidoglycans from Lactobacillus plantarum and Staphylococcus aureus. Molecular immunology 65, 77–85. [PubMed: 25647716]

Barratt MJ, Lebrilla C, Shapiro HY, and Gordon JI (2017). The Gut Microbiota, Food Science, and Human Nutrition: A Timely Marriage. Cell Host Microbe 22, 134–141. [PubMed: 28799899]

Bason JV, Montgomery MG, Leslie AG, and Walker JE (2014). Pathway of binding of the intrinsically disordered mitochondrial inhibitor protein to F1-ATPase. Proceedings of the National Academy of Sciences of the United States of America 111, 11305–11310. [PubMed: 25049402]

Bolz DD, Tenor JL, and Aballay A (2010). A conserved PMK-1/p38 MAPK is required in caenorhabditis elegans tissue-specific immune response to Yersinia pestis infection. The Journal of biological chemistry 285, 10832–10840. [PubMed: 20133945]

Bourhis LL, and Werts C (2007). Role of Nods in bacterial infection. Microbes and infection 9, 629–636. [PubMed: 17379560]

Brandt JP, and Ringstad N (2015). Toll-like Receptor Signaling Promotes Development and Function of Sensory Neurons Required for a C. elegans Pathogen-Avoidance Behavior. Current biology : CB 25, 2228–2237. [PubMed: 26279230]

Brenner S (1974). The genetics of Caenorhabditis elegans. Genetics 77, 71–94. [PubMed: 4366476]

Brown JM, and Hazen SL (2018). Microbial modulation of cardiovascular disease. Nat Rev Microbiol 16, 171–181. [PubMed: 29307889]

Campanella M, Casswell E, Chong S, Farah Z, Wieckowski MR, Abramov AY, Tinker A, and Duchen MR (2008). Regulation of mitochondrial structure and function by the F1Fo-ATPase inhibitor protein, IF1. Cell metabolism 8, 13–25. [PubMed: 18590689]

Cani PD (2018). Human gut microbiome: hopes, threats and promises. Gut 67, 1716–1725. [PubMed: 29934437]

Chin RM, Fu X, Pai MY, Vergnes L, Hwang H, Deng G, Diep S, Lomenick B, Meli VS, Monsalve GC, et al. (2014). The metabolite alpha-ketoglutarate extends lifespan by inhibiting ATP synthase and TOR. Nature 510, 397–401. [PubMed: 24828042]

Coppa A, Guha S, Fourcade S, Parameswaran J, Ruiz M, Moser AB, Schluter A, Murphy MP, Lizcano JM, Miranda-Vizuete A, et al. (2020). The peroxisomal fatty acid transporter ABCD1/PMP-4 is required in the C. elegans hypodermis for axonal maintenance: A worm model for adrenoleukodystrophy. Free radical biology & medicine 152, 797–809. [PubMed: 32017990]

Dingley S, Polyak E, Lightfoot R, Ostrovsky J, Rao M, Greco T, Ischiropoulos H, and Falk MJ (2010). Mitochondrial respiratory chain dysfunction variably increases oxidant stress in Caenorhabditis elegans. Mitochondrion 10, 125–136. [PubMed: 19900588]

Donia MS, and Fischbach MA (2015). HUMAN MICROBIOTA. Small molecules from the human microbiota. Science 349, 1254766. [PubMed: 26206939]

Dunbar TL, Yan Z, Balla KM, Smelkinson MG, and Troemel ER (2012). C. elegans detects pathogen-induced translational inhibition to activate immune signaling. Cell host & microbe 11, 375–386. [PubMed: 22520465]

Esparza-Molto PB, and Cuezva JM (2018). The Role of Mitochondrial H(+)-ATP Synthase in Cancer. Frontiers in oncology 8, 53. [PubMed: 29564224]

Fan Y, and Pedersen O (2020). Gut microbiota in human metabolic health and disease. Nature reviews. Microbiology.

Fernandez-Cardenas LP, Villanueva-Chimal E, Salinas LS, Jose-Nunez C, Tuena de Gomez Puyou M, and Navarro RE (2017). Caenorhabditis elegans ATPase inhibitor factor 1 (IF1) MAI-2 preserves the mitochondrial membrane potential (Deltapsim) and is important to induce germ cell apoptosis. PloS one 12, e0181984. [PubMed: 28829773]

Fischbach MA (2018). Microbiome: Focus on Causation and Mechanism. Cell 174, 785–790. [PubMed: 30096310]

Frakes AE, and Dillin A (2017). The UPR(ER): Sensor and Coordinator of Organismal Homeostasis. Molecular cell 66, 761–771. [PubMed: 28622521]

Garcia-Aguilar A, and Cuezva JM (2018). A Review of the Inhibition of the Mitochondrial ATP Synthase by IF1 in vivo: Reprogramming Energy Metabolism and Inducing Mitohormesis. Frontiers in physiology 9, 1322. [PubMed: 30283362]

Garcia-Bermudez J, Sanchez-Arago M, Soldevilla B, Del Arco A, Nuevo-Tapioles C, and Cuezva JM (2015). PKA Phosphorylates the ATPase Inhibitory Factor 1 and Inactivates Its Capacity to Bind and Inhibit the Mitochondrial H(+)-ATP Synthase. Cell reports 12, 2143–2155. [PubMed: 26387949]

Garcia-Gonzalez AP, Ritter AD, Shrestha S, Andersen EC, Yilmaz LS, and Walhout AJM (2017). Bacterial Metabolism Affects the C. elegans Response to Cancer Chemotherapeutics. Cell 169, 431–441 e438. [PubMed: 28431244]

Girardin SE, Boneca IG, Carneiro LA, Antignac A, Jehanno M, Viala J, Tedin K, Taha MK, Labigne A, Zahringer U, et al. (2003a). Nod1 detects a unique muropeptide from gram-negative bacterial peptidoglycan. Science 300, 1584–1587. [PubMed: 12791997]

Girardin SE, Boneca IG, Viala J, Chamaillard M, Labigne A, Thomas G, Philpott DJ, and Sansonetti PJ. (2003b). Nod2 is a general sensor of peptidoglycan through muramyl dipeptide (MDP) detection. The Journal of biological chemistry 278, 8869–8872. [PubMed: 12527755]

Goldberg J, Currais A, Prior M, Fischer W, Chiruta C, Ratliff E, Daugherty D, Dargusch R, Finley K, Esparza-Molto PB, et al. (2018). The mitochondrial ATP synthase is a shared drug target for aging and dementia. Aging cell 17.

Goodell EW, and Schwarz U (1985). Release of cell wall peptides into culture medium by exponentially growing Escherichia coli. Journal of bacteriology 162, 391–397. [PubMed: 2858468]

Gottar M, Gobert V, Michel T, Belvin M, Duyk G, Hoffmann JA, Ferrandon D, and Royet J (2002). The Drosophila immune response against Gram-negative bacteria is mediated by a peptidoglycan recognition protein. Nature 416, 640–644. [PubMed: 11912488]

Govindan JA, Jayamani E, Zhang X, Mylonakis E, and Ruvkun G (2015). Dialogue between E. coli free radical pathways and the mitochondria of C. elegans. Proceedings of the National Academy of Sciences of the United States of America 112, 12456–12461. [PubMed: 26392561]

Grootjans J, Kaser A, Kaufman RJ, and Blumberg RS (2016). The unfolded protein response in immunity and inflammation. Nature reviews. Immunology 16, 469–484.

Heintz C, and Mair W (2014). You are what you host: microbiome modulation of the aging process. Cell 156, 408–411. [PubMed: 24485451]

Hong S, and Pedersen PL (2008). ATP synthase and the actions of inhibitors utilized to study its roles in human health, disease, and other scientific areas. Microbiology and molecular biology reviews : MMBR 72, 590–641, Table of Contents. [PubMed: 19052322]

Humann J, and Lenz LL (2009). Bacterial peptidoglycan degrading enzymes and their impact on host muropeptide detection. Journal of innate immunity 1, 88–97. [PubMed: 19319201]

Ichikawa N, Ando C, and Fumino M (2006). Caenorhabditis elegans MAI-1 protein, which is similar to mitochondrial ATPase inhibitor (IF1), can inhibit yeast F0F1-ATPase but cannot be transported to yeast mitochondria. Journal of bioenergetics and biomembranes 38, 93–99. [PubMed: 16897438]

Irazoki O, Hernandez SB, and Cava F (2019). Peptidoglycan Muropeptides: Release, Perception, and Functions as Signaling Molecules. Frontiers in microbiology 10, 500. [PubMed: 30984120]

Juan C, Torrens G, Barcelo IM, and Oliver A (2018). Interplay between Peptidoglycan Biology and Virulence in Gram-Negative Pathogens. Microbiology and molecular biology reviews : MMBR 82.

Kitamura M (2013). The unfolded protein response triggered by environmental factors. Seminars in immunopathology 35, 259–275. [PubMed: 23553212]

Kniazeva M, Zhu H, Sewell AK, and Han M (2015). A Lipid-TORC1 Pathway Promotes Neuronal Development and Foraging Behavior under Both Fed and Fasted Conditions in C. elegans. Developmental cell 33, 260–271. [PubMed: 25892013]

Kraus E, and Femfert U (1976). Proteinase K from the mold Tritirachium album Limber. Specificity and mode of action. Hoppe-Seyler's Zeitschrift fur physiologische Chemie 357, 937–947.

Kuhner D, Stahl M, Demircioglu DD, and Bertsche U (2014). From cells to muropeptide structures in 24 h: peptidoglycan mapping by UPLC-MS. Scientific reports 4, 7494. [PubMed: 25510564]

Kundu P, Blacher E, Elinav E, and Pettersson S (2017). Our Gut Microbiome: The Evolving Inner Self. Cell 171, 1481–1493. [PubMed: 29245010]

Labbadia J, and Morimoto RI (2015). The biology of proteostasis in aging and disease. Annual review of biochemistry 84, 435–464.

Lapuente-Brun E, Moreno-Loshuertos R, Acin-Perez R, Latorre-Pellicer A, Colas C, Balsa E, Perales-Clemente E, Quiros PM, Calvo E, Rodriguez-Hernandez MA, et al. (2013). Supercomplex assembly determines electron flux in the mitochondrial electron transport chain. Science 340, 1567–1570. [PubMed: 23812712]

Lee SJ, Hwang AB, and Kenyon C (2010). Inhibition of respiration extends C. elegans life span via reactive oxygen species that increase HIF-1 activity. Current biology : CB 20, 2131–2136. [PubMed: 21093262]

Libina N, Berman JR, and Kenyon C (2003). Tissue-specific activities of C. elegans DAF-16 in the regulation of lifespan. Cell 115, 489–502. [PubMed: 14622602]

Liu Y, Samuel BS, Breen PC, and Ruvkun G (2014). Caenorhabditis elegans pathways that surveil and defend mitochondria. Nature 508, 406–410. [PubMed: 24695221]

MacNeil LT, Watson E, Arda HE, Zhu LJ, and Walhout AJ (2013). Diet-induced developmental acceleration independent of TOR and insulin in C. elegans. Cell 153, 240–252. [PubMed: 23540701]

Magnet S, Bellais S, Dubost L, Fourgeaud M, Mainardi JL, Petit-Frere S, Marie A, Mengin-Lecreulx D, Arthur M, and Gutmann L (2007). Identification of the L,D-transpeptidases responsible for attachment of the Braun lipoprotein to Escherichia coli peptidoglycan. Journal of bacteriology 189, 3927–3931. [PubMed: 17369299]

Mann B, Loh LN, Gao G, and Tuomanen E (2016). Preparation of Purified Gram-positive Bacterial Cell Wall and Detection in Placenta and Fetal Tissues. Bio-protocol 6.

McDonald C, Inohara N, and Nunez G (2005). Peptidoglycan signaling in innate immunity and inflammatory disease. The Journal of biological chemistry 280, 20177–20180. [PubMed: 15802263]

Meisel JD, Panda O, Mahanti P, Schroeder FC, and Kim DH (2014). Chemosensation of bacterial secondary metabolites modulates neuroendocrine signaling and behavior of C. elegans. Cell 159, 267–280. [PubMed: 25303524]

Melo JA, and Ruvkun G (2012). Inactivation of conserved C. elegans genes engages pathogen- and xenobiotic-associated defenses. Cell 149, 452–466. [PubMed: 22500807]

Mitra S, and Ryoo HD (2019). The unfolded protein response in metazoan development. Journal of cell science 132.

Packiam M, Weinrick B, Jacobs WR Jr., and Maurelli AT (2015). Structural characterization of muropeptides from Chlamydia trachomatis peptidoglycan by mass spectrometry resolves "chlamydial anomaly". Proceedings of the National Academy of Sciences of the United States of America 112, 11660–11665. [PubMed: 26290580]

Palaniyar N, Nadesalingam J, and Reid KB (2002). Pulmonary innate immune proteins and receptors that interact with gram-positive bacterial ligands. Immunobiology 205, 575–594. [PubMed: 12396017]

Park JT, and Uehara T (2008). How bacteria consume their own exoskeletons (turnover and recycling of cell wall peptidoglycan). Microbiology and molecular biology reviews : MMBR 72, 211–227, table of contents. [PubMed: 18535144]

Postler TS, and Ghosh S (2017). Understanding the Holobiont: How Microbial Metabolites Affect Human Health and Shape the Immune System. Cell Metab 26, 110–130. [PubMed: 28625867]

Pullman ME, and Monroy GC (1963). A Naturally Occurring Inhibitor of Mitochondrial Adenosine Triphosphatase. The Journal of biological chemistry 238, 3762–3769. [PubMed: 14109217]

Qi B, and Han M (2018). Microbial Siderophore Enterobactin Promotes Mitochondrial Iron Uptake and Development of the Host via Interaction with ATP Synthase. Cell 175, 571–582 e511. [PubMed: 30146159]

Qi B, Kniazeva M, and Han M (2017). A vitamin-B2-sensing mechanism that regulates gut protease activity to impact animal's food behavior and growth. eLife 6.

Royet J, Gupta D, and Dziarski R (2011). Peptidoglycan recognition proteins: modulators of the microbiome and inflammation. Nature reviews. Immunology 11, 837–851.

Sanders AN, and Pavelka MS (2013). Phenotypic analysis of Eschericia coli mutants lacking L,D-transpeptidases. Microbiology 159, 1842–1852. [PubMed: 23832002]

Schleifer KH, and Kandler O (1972). Peptidoglycan types of bacterial cell walls and their taxonomic implications. Bacteriological reviews 36, 407–477. [PubMed: 4568761]

Schulenburg H, and Boehnisch C (2008). Diversification and adaptive sequence evolution of Caenorhabditis lysozymes (Nematoda: Rhabditidae). BMC evolutionary biology 8, 114. [PubMed: 18423043]

Shpilka T, and Haynes CM (2018). The mitochondrial UPR: mechanisms, physiological functions and implications in ageing. Nature reviews. Molecular cell biology 19, 109–120. [PubMed: 29165426]

Shtonda BB, and Avery L (2006). Dietary choice behavior in Caenorhabditis elegans. The Journal of experimental biology 209, 89–102. [PubMed: 16354781]

Taylor RC, Berendzen KM, and Dillin A (2014). Systemic stress signalling: understanding the cell non-autonomous control of proteostasis. Nature reviews. Molecular cell biology 15, 211–217.

Typas A, Banzhaf M, Gross CA, and Vollmer W (2011). From the regulation of peptidoglycan synthesis to bacterial growth and morphology. Nature reviews. Microbiology 10, 123–136. [PubMed: 22203377]

Uehara T, Dinh T, and Bernhardt TG (2009). LytM-domain factors are required for daughter cell separation and rapid ampicillin-induced lysis in Escherichia coli. Journal of bacteriology 191, 5094–5107. [PubMed: 19525345]

van Heijenoort J (2011). Peptidoglycan hydrolases of Escherichia coli. Microbiology and molecular biology reviews : MMBR 75, 636–663. [PubMed: 22126997]

Vollmer W, and Holtje JV (2004). The architecture of the murein (peptidoglycan) in gram-negative bacteria: vertical scaffold or horizontal layer(s)? Journal of bacteriology 186, 5978–5987. [PubMed: 15342566]

Zhang J, Li X, Olmedo M, Holdorf AD, Shang Y, Artal-Sanz M, Yilmaz LS, and Walhout AJM (2019). A Delicate Balance between Bacterial Iron and Reactive Oxygen Species Supports Optimal C. elegans Development. Cell host & microbe 26, 400–411 e403. [PubMed: 31444089]

Zhang L, Gualberto DG, Guo X, Correa P, Jee C, and Garcia LR (2015). TMC-1 attenuates C. elegans development and sexual behaviour in a chemically defined food environment. Nature communications 6, 6345.

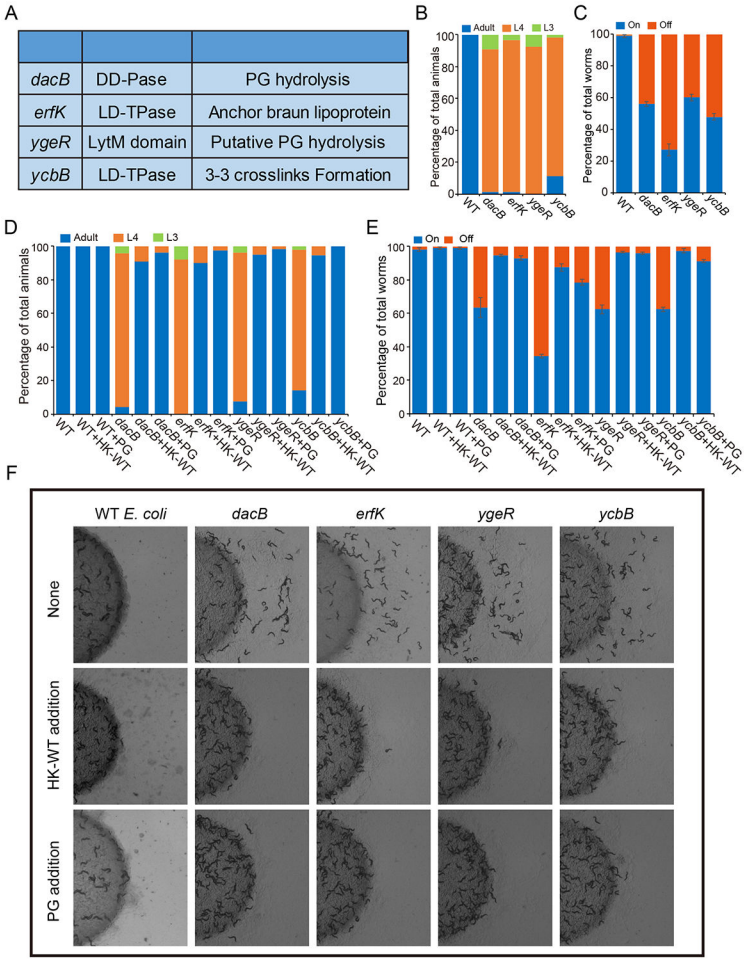

Figure 1. Peptidoglycan (PG) from *E. coli* is required for the development and food behavior in *C. elegans*

(A) List of 4 *E. coli* PG metabolic genes identified in a screen of the Keio mutant collection (*E. coli* K-12). DD-Pase, DD-carboxypeptidase and DD-endopeptidase; LD-TPase, LD-transpeptidase (Typas et al., 2011; van Heijenoort, 2011).

(B) Bar graph showing worms fed each of 4 PG mutants displayed growth delay as indicated by percentage of worms at the indicated developmental stages. Larval stages were visually determined based on vulval development. n = 53-140.

(C) Worms fed with each of 4 PG mutants exhibited food avoidance behavior. Data are presented as the percentage of worms found On or Off the bacterial lawn. 100-200 animals/assay. Data are represented as mean ± SEM from three replicates.

(D-F) Bar graphs and representative microscope images showing that both the growth delay (D, n = 49-78) and food avoidance (E and F, 100-200 animals/assay, mean ± SEM from three replicates) phenotypes were suppressed by adding heat-killed wild type K-12 bacteria (HK-WT) or isolated PG.

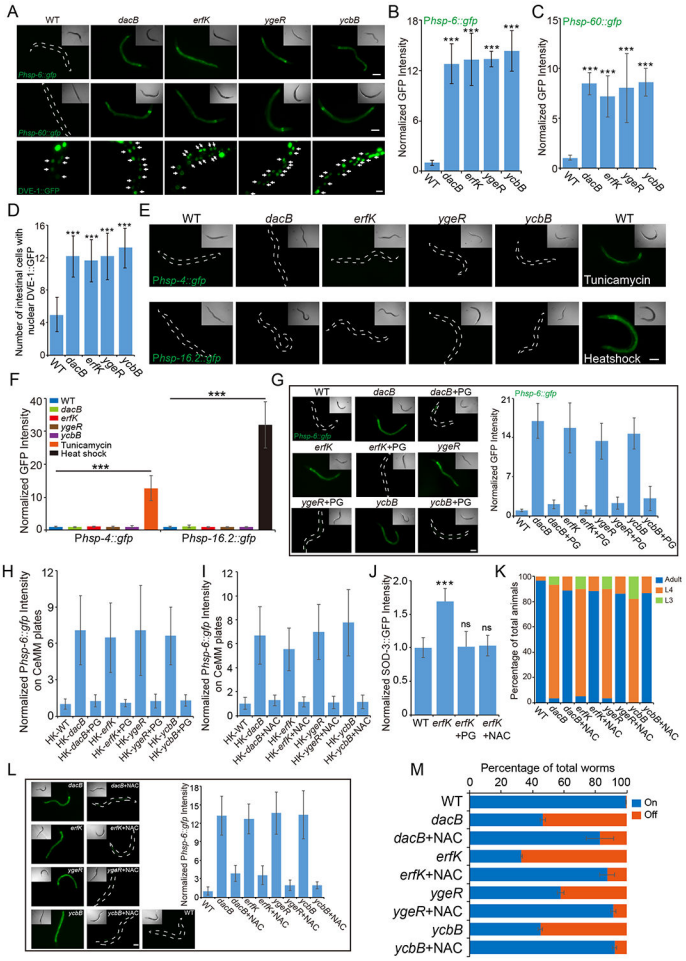

Figure 2. Absence of beneficial PG metabolites induces Mt stress in *C. elegans*

(A-D) GFP fluorescence images and bar graphs showing that feeding each of the 4 PG mutant *E. coli* induced Mt stress as indicated by Mt stress/UPR^{mt} reporters (P*hsp-6::gfp* and P*hsp-60::gfp*), and nuclear accumulation of DVE-1::GFP in the intestine. n = 31-68 in (B), n = 31-32 in (C), and n = 39-40 in (D). Error bars: mean ± SD. Scale bar, 100 μm for the top and middle panels in (A), 20 μm for the bottom panels in (A).

(E and F) GFP fluorescence images and bar graph showing PG mutant diet did not trigger ER stress (P*hsp-4::gfp*, n = 27-37, mean ± SD) or cytoplasmic stress (P*hsp-16.2::gfp*, n = 32-36, mean ± SD). Tunicamycin (n = 29) and heat shock (n = 32) were used as positive controls for ER stress and cytoplasmic stress, respectively. Scale bar in (E), 100 μm.

(G) GFP images and bar graph showing PG isolated from wild type *E. coli* suppressed Mt stress (P*hsp-6::GFP*) induced by feeding each of the 4 PG mutant *E. coli* (n = 30-37, mean ± SD). Scale bar, 100 μm.

(H and I) Bar graphs showing that, in the germ-free CeMM medium, heat-killed *E. coli* of each of the four PG mutants induced a high-level Mt stress (Phsp-6::GFP) relative to the level by heat-killed wild type *E. coli* and such induced-Mt stress was effectively suppressed by supplementing either PG isolated from wild-type *E. coli* or antioxidant NAC. n = 20-25. Representative images are shown in Figure S3E and S3G.

(J) Feeding *erfK* mutant *E. coli* upregulated the level of SOD-3::GFP and the increase was suppressed by adding PG from wild type *E. coli* or NAC. (n = 29-30, mean ± SD). The results from tests done in the germ-free CeMM medium is shown in Figure S3I
(K-M), Bar graphs and representative microscope images showing that NAC supplementation suppressed growth delay (K, n = 52-61), Mt stress (L, n = 20-23) and food avoidance behavior (M, 100-200 animals/assay, mean ± SEM from 3 replicates). Scale bar in (L), 100 μm. Representative images for (M) is shown in Figure S3J.
*** $p<0.001$, ns: not significant.

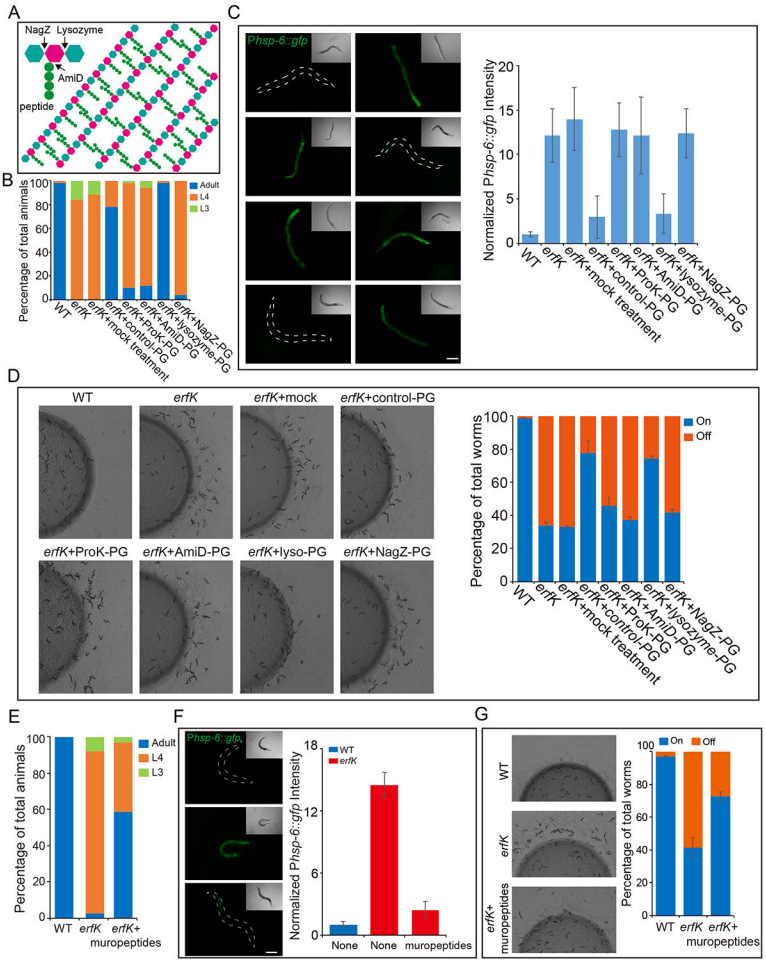

Figure 3. Beneficial muropeptides contain disaccharides and short peptides

(A) Cartoon diagram of a large PG molecule and the cleavage points of 3 enzymes indicated by black arrows. NagZ: Glucosaminidase; AmiD: Amidase; NAG: 3' *N*-acetylglucosamine; NAM: 5' *N*-acetylmuramic acid.

(B-D) Bar graphs and microscope images showing the effects of treating isolated PG with the indicated enzymes. ProtesaseK (ProK), AmiD or NagZ treated PG failed to suppress the growth delay (B, n = 50-59), Mt stress (C, n = 30-31, mean ± SD) or food avoidance (D, 100-200 animals/assay, mean ± SEM from 3 replicates) phenotypes in animals fed the *erfK* mutant *E. coli*. PG and lysozyme (lyso) treated PG suppressed all three phenotypes.

(E-G) Muropeptides isolated from lysozyme-treated PG suppressed growth delay (E, n = 30-65), Mt stress (F, n = 30-32, mean ± SD) and food avoidance (G, 100-200 animals/assay, mean ± SEM from 3 replicates). Scale bar in (C) and (F), 100 μm.

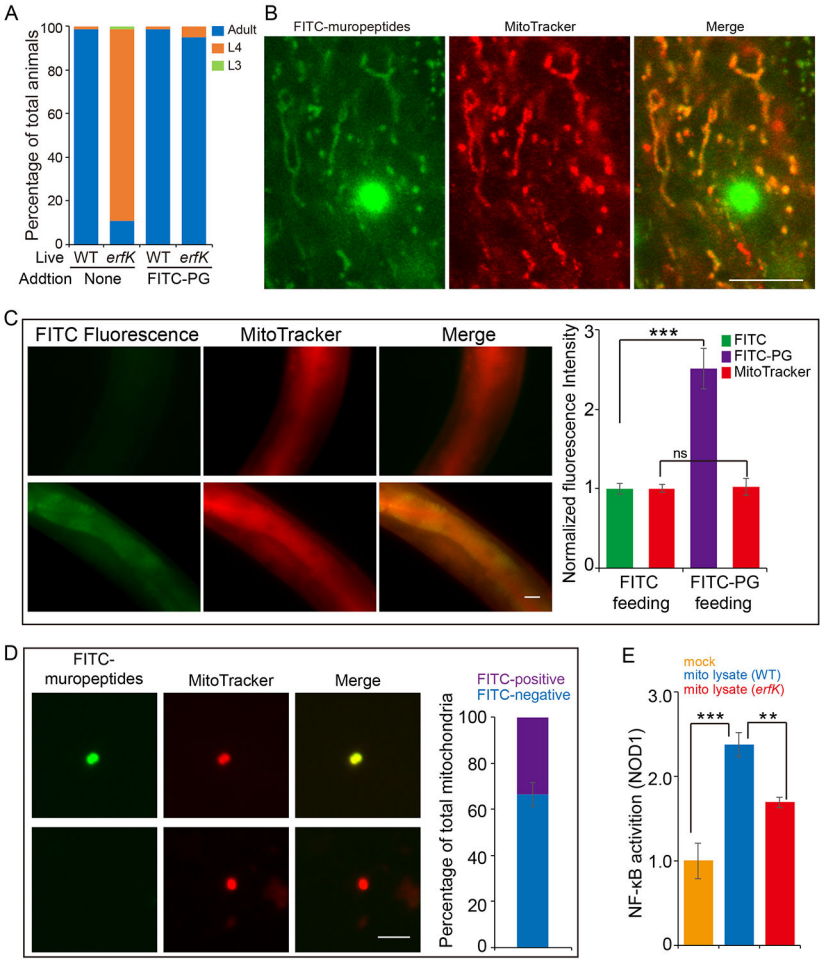

Figure 4. Muropeptides enter and accumulate in host intestinal mitochondria

(A) FITC labeled PG (FITC-PG) suppressed the growth defect of worms fed *erfK* mutant *E. coli* (n = 64-80).

(B) Representative fluorescent images showing in vivo co-localization of FITC-muropeptides and MitoTracter in worm mitochondria (arrows). The arrowheat indicates an auto-fluorescent granule. Scale bar: 10μm.

(C) Representative images and quantitative data showing FITC-muropeptide accumulation in intestinal cells of *C. elegans* that were also fed with MitoTracker as a control. Animals were fixed to remove intestinal auto-fluorescence. n = 17-18, mean ± SD. Scale Bar: 100μm.

(D) Representative images and quantitative data showing co-localization of FITC-muropeptides and MitoTracker in a subset of isolated Mt (FITC-positive Mt in upper panel). Quantification showing that 34% of total isolated Mt are FITC-positive, 66% are FITC-negative. FITC-positive Mt may be derived from intestinal cells while FITC-negative Mt may represent Mt from non-intestinal cells. Mean ± SEM, n = 336 from 3 replicates. Scale bar: 5μm.

(E) Data from an NF-κB activity assay that indicates the interaction between muropeptides from *C. elegans* Mt lysates and NOD-1 in mammalian cells. Mt lysate from worms fed wild-type *E. coli* induced higher NF-κB activity than the lysate from worms fed *erfK* mutant *E. coli*. Mean ± SEM from 3 replicates.

*** p<0.001, ** p<0.01.

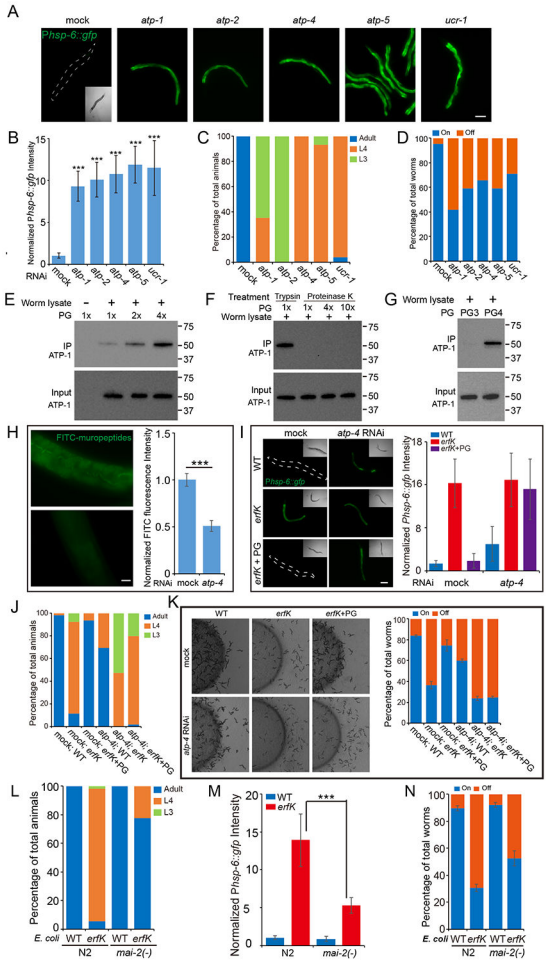

Figure 5. Muropeptides bind to ATP synthase in the host for the beneficial function

(A-D) RNAi knockdown of 5 PG interactor candidates triggered Mt stress (A and B, n = 33-37, mean ± SD), growth delay (C, n = 49-60) and food avoidance behavior (D, 100-200 animals/assay, mean ± SEM from 3 replicates). (Representative images for D are shown in Figure S5B). Scale bar in (A) is 100 μm.

(E) Interaction between PG and ATP-1 detected by *in vivo* pull-down assays. ATP-1 from worm lysates was bound to PG and the binding increased in a concentration dependent manner.

(F) Proteinase-K treatment (to which short peptides on PG are sensitive), but not trypsin treatment (to which the short amino acid peptides on PG are insensitive), eliminated the binding of PG to ATP-1.

(G) Trypsin treatment in Step 4 of the PG purification procedure (Figure S3A), which is expected to remove lipoproteins attached to PG, is required for PG to pull down ATP-1 from worm lysates.

(H) GFP images and bar graph showing that the level of FITC-muropeptides in intestinal cells was decreased in *atp-4* RNAi knockdown animals. Animals were fixed to remove intestinal autofluorescence. n = 31, mean ± SEM.

(I-K) Representative images and bar graphs showing the dependence of the beneficial role of PG on ATP synthase. In *atp-4* RNAi knockdown animals, addition of PG failed to suppress

Mt stress (I, n = 30-34, mean ± SD), growth delay (J, n = 53-62) and food avoidance behavior (K, 100-200 animals/assay, mean ± SEM from 3 replicates) when feeding with *erfK* mutant *E. coli*. *atp-4i = atp-4* RNAi treatment. Scale bar in (H), 5 μm; in (I), 100 μm. (L-N) Bar graphs showing that growth delay (L, n = 54-62), Mt stress (M, n = 30-34, mean ± SD) and food avoidance behavior (N, 100-200 animals/assay, mean ± SEM from 3 replicates) in worms fed *erfK* mutant *E. coli* were partially suppressed by the *mai-2(−)* mutation, *mai-2(xm19)*.

*** $p<0.001$.

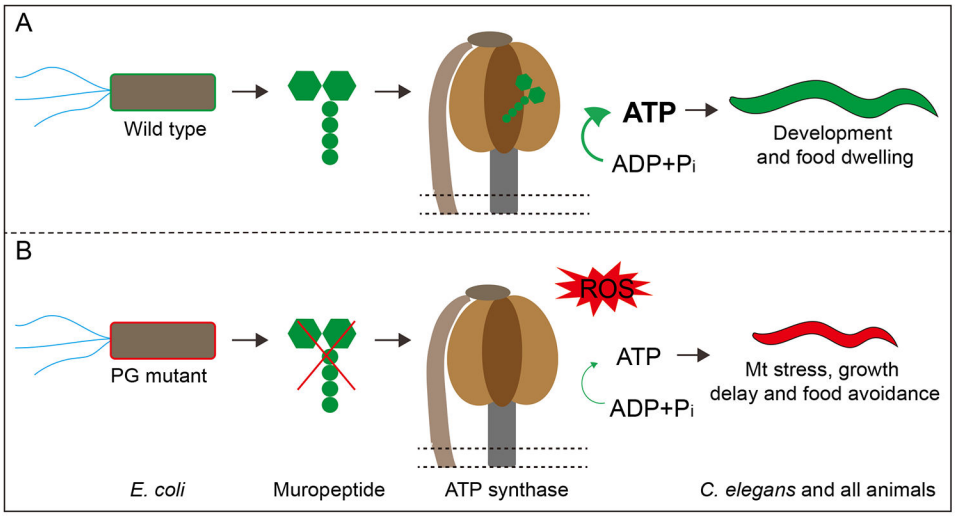

Figure 6. A model for the beneficial role of bacterial muropeptides in host animals

(A) *E. coli*-produced disaccharide muropeptides act as an ATP synthase agonist by entering host Mt and binding to ATP synthase to promote its activity. The increased ATP synthesis promotes Mt homeostasis, host development and food dwelling behavior in *C. elegans.* (B) Lack of muropeptides (PG mutant *E. coli* feeding or germ-free condition) inhibits ATP synthase activity and increases ROS production. The decreased ATP synthesis trigger Mt stress, growth delay and food avoidance behavior in *C. elegans*. Given that bacterial muropeptides are known to enter cells in mammals and the structure of ATP synthase is exceedingly conserved, such a beneficial role of muropeptides is likely conserved in mammals.

Key resources table

REAGENT or RESOURCE	SOURCE	IDENTIFIER
Antibodies		
ATP5A1 Monoclonal Antibody (15H4C4)	Thermo Fisher Scientific	Cat #43-9800 RRID:AB_2533548
Anti-mouse IgG, HRP linked Antibody	Cell Signaling Technology	Cat#7076S;RRID:AB_330924
Bacterial and virus strains		
E. coli Keio Knockout Parent Strain BW25113	Dharmacon	Cat #OEC5042
E. coli Keio Knockout Collection	Dharmacon	Cat #OEC4988
Escherichia coli OP50	*Caenorhabditis* Genetics Center (CGC)	RRID:WB-STRAIN:OP50
RNAi feeding bacterial strain HT115(DE3)	Dharmacon	N/A
C.elegans ORF RNAi library Collection	Dharmacon	Car#RCE1181
Chemicals, peptides, and recombinant proteins		
CeMM reagents	Table S3	Table S3
Deoxyribonuclease I	Sigma	Cat #DN25
Ribonuclease A	Sigma	Cat #R4875
Trypsin	Sigma	Cat #T1426
Tunicamycin	Thermo Fisher Scientific	Cat #ICN15002801
H2DCFDA	Thermo Fisher Scientific	Cat #59-351-00
lysozyme	Thermo Fisher Scientific	Cat# 44-031-GM
Proteinase K	Sigma	Cat # P2308
Fluorescein Isothiocyanate Isomer I (FITC)	Thermo Fisher Scientific	Cat #AC119252500
Iron(III) chloride hexahydrate	Sigma	Cat #236489
MitoTracker Red CMXRos	Cell Signaling Technology	Cat #9082S
Halt™ Protease Inhibitor Cocktail	Thermo Fisher Scientific	Cat # PI87786
N-acetyl-L-cysteine	Thermo Fisher Scientific	Cat # ICN10009825
E.coli NagZ Recombinant protein (12xHis-tagged)	This study	N/A
E.coli AmiD Recombinant protein (12xHis-tagged)	This study	N/A
Critical commercial assays		
Mitochondria Isolation Kit for Tissue	Thermo Fisher Scientific	Cat #89801
HEK-Blue™ hNOD1	Invivogen	Cat# hkb-hnod1
ECL Prime Western Blotting kit	GE Healthcare	Cat #RPN2232
Experimental models: Cell lines		
human NOD1-expressing HEK 293 cells	Invivogen	Cat# 293-hnod1
Experimental models: Organisms/strains		
C. elegans: N2	*Caenorhabditis* Genetics Center (CGC)	N/A
C. elegans: Strain: SJ4100: *zcIs13[Phsp-6::gfp] V*	*Caenorhabditis* Genetics Center (CGC)	N/A
C. elegans: Strain: SJ4058: *zcIs9[Phsp-60::gfp + lin-15(+)] V*	*Caenorhabditis* Genetics Center (CGC)	N/A

REAGENT or RESOURCE	SOURCE	IDENTIFIER
C. elegans: Strain: SJ4197: *zcIs39[Pdve-1::dve-1::gfp] II*	*Caenorhabditis* Genetics Center (CGC)	N/A
C. elegans: Strain: SJ4005: *zcIs4 [Phsp-4::gfp] V*	*Caenorhabditis* Genetics Center (CGC)	N/A
C. elegans: Strain: TJ375: *gpIs1 [Phsp-16.2::gfp]*	*Caenorhabditis* Genetics Center (CGC)	N/A
C. elegans: Strain: AY101: *acIs101 [PF35E12.5::gfp + rol-6(su1006)]*	*Caenorhabditis* Genetics Center (CGC)	N/A
C. elegans: Strain: AU133: *agIs17 [Pmyo-2::mCherry + Pirg-1::gfp] IV*	*Caenorhabditis* Genetics Center (CGC)	N/A
C. elegans: Strain: CF1553: *muIs84 [(pAD76) sod-3p::GFP + rol-6(su1006)]*	*Caenorhabditis* Genetics Center (CGC)	N/A
C. elegans: Strain:RN71: *mai-2(xm19); bcIs39 V*	(Fernandez-Cardenas et al., 2017)	N/A
C. elegans: Strain:MH6036: *mai-2(xm19)*	This study	N/A
C. elegans: Strain:MH6037 *mai-2(xm19) zcIs13[Phsp-6::gfp] V)*	This study	N/A
Oligonucleotides		
dacB forward: CGTAAGGTCATCGGAATAGCTTGC	This study	N/A
dacB reverse: AAGACGACGAAGAAGGCGTTGAGT	This study	N/A
erfK forward:GTATCTCATTCCTTCTCACCTGTCGG	This study	N/A
erfK reverse: ATGCACCACGATGGTTCATTACCC	This study	N/A
ygeR forward: GGAGGTAGGAAGTGTGATGACGTT	This study	N/A
ygeR reverse ATCGAACCCTCGTATAGAGCTTGG	This study	N/A
ycbB forward AGCCTGATGAGTAACAGGCTTGCT	This study	N/A
ycbB reverse TCCTGAATATAGCCTCTGCCATCG	This study	N/A
K1 reverse: CAGTCATAGCCGAATAGCCT	(Baba et al., 2006)	N/A
K2 forward: CGGTGCCCTGAATGAACTGC	(Baba et al., 2006)	N/A
Recombinant DNA		
Plasmid: pET28a-12xHis-NagZ	This study	N/A
Plasmid: pET28a-12xHis-AmiD	This study	N/A
Software and algorithms		
ImageJsoftware	NIH	https://imagej.nih.gov/ij/